

POSITION-AGNOSTIC MULTI-MICROPHONE SPEECH DEREVERBERATION

Yochai Yemini¹, Ethan Fetaya¹, Haggai Maron² and Sharon Gannot¹

¹Faculty of Engineering, Bar-Ilan University, Ramat-Gan, 5290002, Israel ²NVIDIA Research
{Yochai.Yemini, Ethan.Fetaya, Sharon.Gannot}@biu.ac.il; hmaron@nvidia.com

ABSTRACT

Neural networks (NNs) have been widely applied in speech processing tasks, and, in particular, those employing microphone arrays. Nevertheless, most of the existing NN architectures can only deal with fixed and position-specific microphone arrays. In this paper, we present an NN architecture that can cope with microphone arrays on which no prior knowledge is presumed, and demonstrate its applicability on the speech dereverberation problem. To this end, our approach harnesses recent advances in the Deep Sets framework to design an architecture that enhances the reverberant log-spectrum. We provide a setup for training and testing such a network. Our experiments, using REVERB challenge datasets, show that the proposed position-agnostic setup performs comparably with the position-aware framework and sometimes slightly better, even with fewer microphones. In addition, it substantially improves performance over a single microphone architecture.

Index Terms— Speech dereverberation, deep neural network, deep sets, microphone array

1. INTRODUCTION

As a sound wave propagates in an acoustic enclosure, it reflects from the room's facets and from the objects within the room. A microphone in that room will capture both the direct path signal and the associated reflections. This phenomenon, known as reverberation, negatively impacts speech quality and, in severe cases, even its intelligibility [1], posing difficulties to hearing impaired people as well as automated speech recognition (ASR) systems. With the soaring popularity of ASR based agents such as Amazon Alexa, Microsoft Cortana and Google Siri, mitigating reverberation is further incentivised.

In many cases, we have access to several audio signals that were captured by different microphones. Importantly, having access to several recordings of the same audio signal enables algorithms to reinforce spectral cues with spatial information, leading to better results compared to the single microphone case. For approaches that require a training stage, we distinguish between two multiple microphone setups: (1) In a *position-aware setup* the relative positions of the microphones are constant and known, e.g. a fixed microphone array

(2) In a *position-agnostic setup* we do not have any prior information on the relative positions of the microphones. For example, this is the case when several different people capture the same audio signal spontaneously at a concert or a lecture [2].

In general, traditional speech processing algorithms are designed to deal with both position-aware and position agnostic scenarios. In the context of speech dereverberation, a plethora of methods exists [3, 4]. One approach, for instance, uses a filter estimation scheme: in the short-time Fourier transform (STFT) domain, reverberation can be modelled as a convolution along frames between the clean STFT and a reverberation filter, independently for each frequency. In [5], the inverse of the filter is estimated by minimising the weighted linear prediction error (WPE). In [6], the authors follow a recursive expectation-maximization paradigm to directly estimate the reverberation filters and to dereverberate the signal using the Kalman filter algorithm. A different approach [7, 8] deploys a late reverberation analysis to devise a dereverberation system.

In this paper we tackle the position agnostic setup for neural network based algorithms. The network takes as input several distorted audio signals represented as log-spectra and our task is to predict a single high quality spectrogram of the underlying audio signal. The main challenge here is devising a neural network architecture that is suitable for our scenario. We have two main requirements: first, we would like the architecture to be *invariant* to the order of the signals; second, we would like the architecture to respect the image-like structure of the spectrograms, for being capable of reconstructing complex structures such as the pitch.

Previous approaches successfully dealt with only one of these requirements: for example, the multi-microphone setup is often dealt with by concatenating the per microphone STFT along the channel axis [9, 10, 11]. This approach is useful when the array geometry is fixed. However, when the microphones are not anchored and may change their respective geometry and position, a simplistic concatenation creates a mismatch with respect to the training data. A recent line of studies has taken steps to mitigate this problem by adopting the deep sets [12] paradigm for speech separation, e.g. [13, 14].

In this contribution, dereverberation is carried out via log-spectrum enhancement while the phase remains unaltered,

rendering the problem an image-like estimation. To address both challenges mentioned above, we leverage a recently suggested architecture for learning sets of symmetric elements [15]. This framework captures both the set symmetry and the intrinsic symmetries of each element in the set by replacing convolution layers with deep symmetric sets (DSS) layers.

To demonstrate the efficacy of our approach we provide an extensive experimental evaluation on the REVERB dataset [4], including newly designed train-test splits that focus on the position-agnostic setup. In this setup we train on several microphone configurations and test on unseen combinations.

2. PROBLEM FORMULATION

Let $x(t)$ denote the anechoic signal in the discrete-time domain. The reverberant signal can be described as the convolution between $x(t)$ and the reverberant room impulse response (RIR). Therefore, given a microphone array with M microphones, the received signal at each microphone is

$$y_i(t) = \{x * h_i\}(t) + n_i(t), \quad i = 1, 2, \dots, M \quad (1)$$

where $h_i(t)$ and $n_i(t)$ are the per microphone RIR and low-level stationary noise, respectively. The objective is to estimate $x(t)$ given the corrupted observations $\{y_i(t)\}_{i=1}^M$.

To achieve this goal, the signals are first transformed to the log-spectrum representation. Let $Y_i(n, k)$ denote the log-spectrum of $y_i(t)$, i.e. the log-absolute value of the STFT of $y_i(t)$ at the n -th frame and the k -th frequency bin, where $k = 0, 1, \dots, K - 1$. Due to the symmetry of the discrete Fourier transform (DFT), only the first $K/2 + 1$ frequency elements are considered. Denote $F = K/2$. For brevity, the time and frequency indices will be omitted when they are unnecessary for the clarity of the paper.

In this work, a neural network is used to predict X , the log-spectrum of the clean signal. After the enhanced log-spectrum is obtained, it is transformed back to the time domain using the noisy phase of the STFT from the arbitrarily chosen first microphone. Invariance in this context means that the network’s output remains the same for any permutation of $\{Y_i\}_{i=1}^M$, although it is not invariant with respect to the phase. Note that naïve concatenation of the multi-microphone input along the channel axis of the network does not guarantee any sort of invariance, thus unsuitable for position-agnostic processing.

3. ALGORITHM

The proposed method is inspired by several studies. It is based on dereverberation via image deblurring in the log-spectrum domain [16] using a U-net architecture [17] that estimates a clean spectrogram directly from the reverberated one. This approach demonstrated promising results, surpassing several baselines by a significant margin. We extend it to the multi-microphone case by deploying the powerful burst

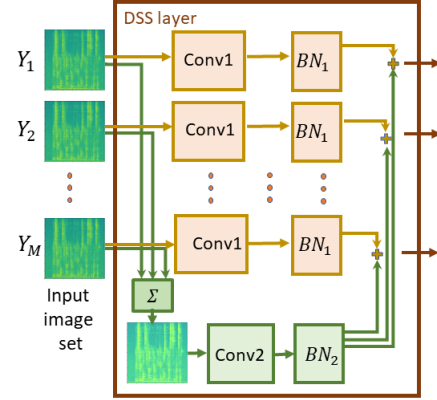


Fig. 1: The DSS layer [15] used in this work, composed of a Siamese network applied independently to each image and an aggregation branch, realised as a sum operation. The Siamese network and the aggregation branch use distinct convolution and batch-normalisation (BN) layers.

image deblurring framework [18], which takes in a set of blurry images and outputs a clean image. A U-net architecture with DSS layers [15] serves as our network of choice. The invariance property of the DSS layer allows the network to process ad hoc distributed microphone arrays, in addition to fixed geometry arrays.

Preprocessing: For a given set of reverberant time-domain samples $\{y_i(t)\}_{i=1}^M$, a preprocessing step first normalises the root-mean-square (RMS) across all M signals to a constant value of 0.1. Then, the log-spectra images $\{Y_i\}_{i=1}^M$ are computed. The M log-spectra are divided to slices of 256 frames each, resulting in multiple slices of size $M \times 1 \times 256 \times (F + 1)$, where the second dimension signifies the channel axis. Since the highest frequency alone does not carry much information, and for computational reasons, it is not enhanced. The M images of size $1 \times 256 \times F$ are linearly mapped to the range $[-1, 1]$, which makes learning faster and more stable.

Network Architecture: Our network receives the $M \times 1 \times 256 \times F$ input, and predicts an output of size $1 \times 256 \times F$. After all slices have been enhanced, the estimated log-spectrum \hat{X} is constructed by concatenating the enhanced slices along the time axis and then mapping the range $[-1, 1]$ back to the valid range of a spectrogram. Eventually, the highest frequency is reattached. As mentioned, the proposed network is based on a U-net network and DSS layers. Each DSS layer receives and outputs a set of M images (Fig. 1). Similarly to [16], the U-net compresses the spatial resolution of the input images to 1×1 , and then unrolls it back to the original resolution of $256 \times F$.

Implementation Details: The following notations are used to describe the network. A $D_{d/u,n}$ layer denotes a DSS layer that comprises strided convolutions with a down/upsampling factor of 2 and has n filters. L and R mark a LeakyReLU activation with a negative slope of 0.2 and a ReLU activation,

respectively. All convolution layers use 4×4 kernels. The encoder’s layers are:

$D_{d,64}L \rightarrow D_{d,128}L \rightarrow D_{d,256}L \rightarrow D_{d,512}L \rightarrow D_{d,512}L \rightarrow D_{d,512}L \rightarrow D_{d,512}L \rightarrow D_{d,512}L$ and the decoder’s architecture is $D_{u,512}R \rightarrow D_{u,512}R \rightarrow D_{u,512}R \rightarrow D_{u,512}R \rightarrow D_{u,256}R \rightarrow R_{u,128}R \rightarrow D_{u,64}R \rightarrow D_{u,1}R$. Skip connections are added between the encoder and decoder to form the U-net part of the network. At the decoder’s output, the dimensions are $M \times 1 \times 256 \times F$. In order to reach a set-based result, a max pooling layer is applied along the set dimension [18], highlighting the dominant features. Eventually the network terminates with $CBR \rightarrow CT$, where C is a convolution layer with stride 1 and a single output channel, B stands for a BN layer and T is the Tanh activation.

Unlike [16], we only use square filters and do not incorporate any generative adversarial network (GAN) framework such as Pix2Pix [19]. Based on [16], it makes the training more intricate while not resulting in substantial improvement.

We train using a loss that also incorporates the error in the gradients, similarly to [18]

$$\text{GradLoss}(\mathbf{Z}, \hat{\mathbf{Z}}) = \frac{1}{10} \|\mathbf{Z} - \hat{\mathbf{Z}}\|_2^2 + \|\nabla \mathbf{Z} - \nabla \hat{\mathbf{Z}}\|_2^2. \quad (2)$$

Here $\hat{\mathbf{Z}}$ and \mathbf{Z} are the network’s prediction and the target, respectively, and ∇ denotes the horizontal and vertical finite differences. The second term encourages the edges of the output image to be similar to those of the target image.

4. EXPERIMENTAL STUDY

Data: The dataset used for training and evaluation is described in the REVERB Challenge [4]. It consists of simulated and real recordings, acquired by an eight-channel circular array with a 20 cm diameter. The former simulates speech sources in three different rooms, corresponding to reverberation times (T_{60}) of 0.25s, 0.5s, and 0.7s. For each room, two speaker-array constellations were considered, i.e. near source (50 cm) or far source (200 cm). Speech sources were generated using clean utterances drawn from the WSJCAM0 dataset [20] convolved with simulated RIRs. A stationary noise (air conditioning) was added to the reverberant speech with a signal-to-noise ratio (SNR) of 20 dB. The speaker may change positions between different utterances. The real, noisy and reverberant speech recordings were collected from a meeting room, different from the simulated rooms, with T_{60} of 0.7s. The clean utterances were drawn from the MC-WSJ-AV corpus [21]. The distance between the speech source and the array, was either 100 cm or 250 cm.

All audio signals were sampled at 16KHz. For calculating the STFT, a Hanning window with $K = 512$ and 75% overlap between successive frames were used for analysis and synthesis. During training, slices of size $256 \times F$ are randomly sampled from the reverberant log-spectrum across the M microphones together with the corresponding slice from the clean

spectrogram. In order to confine the clean and noisy spectrograms to $[-1, 1]$, the minimum and maximum values over the entire training dataset are calculated before the training stage. These values are also used to map the network’s output back to the legitimate range of values of a clean spectrogram.

Experimental setup: We train and test our network under two setups, that address the position-aware and the position-agnostic cases. In the position-aware regime, the network is trained and tested on one fixed subset of microphones. To investigate the position-agnostic scenario, we randomly select a subset of microphones in each iteration. When $n < M$ microphones are used, 70% of the $\binom{M}{n}$ configurations are used for training and other 30% unseen configurations are used for evaluation.

Baselines and evaluation criteria: The criteria used for comparison are cepstral distance (CD), perceptual evaluation of speech quality (PESQ) and frequency weighted segmental SNR (FWSegSNR). As the proposed technique formulates speech dereverberation as an image deblurring problem, and due to limited space, it is primarily compared against [16]. For the position-aware setup, we also trained a network identical to [16] that concatenates the multi-microphone input. However, the objective benchmarks were not impressive and due to space constraints are not presented here. We hypothesize that the DSS based architecture is more successful since it allows each microphone to be processed independently (while being exposed to all other microphones). More comprehensive comparisons will be presented in a follow-up work. We used our own implementation of the network described in [16], and trained it with GradLoss. The achieved results were slightly better than those reported in [16]. Note that since each DSS layer uses two convolutions layers, our network has twice as many parameters compared to [16]. For fairness, we also evaluated [16] with the same number of parameters as our network’s and verified that the results are consistent.

Discussion: Tables 1 and 2 provide the quantitative results for the simulated recordings. The position-aware case was evaluated on one, four and eight microphones, and the position-agnostic sets on two, four and six. As can be seen, for both near and far microphones the performance consistently improves with the number of microphones across all benchmarks. In most cases, the best results are achieved with eight microphones. Nonetheless, we note that in spite of using fewer microphones, the position-agnostic sets scheme performs almost on par or even better than the fixed sets counterpart. This is remarkable considering that position-agnostic sets are tested on unseen microphone combinations.

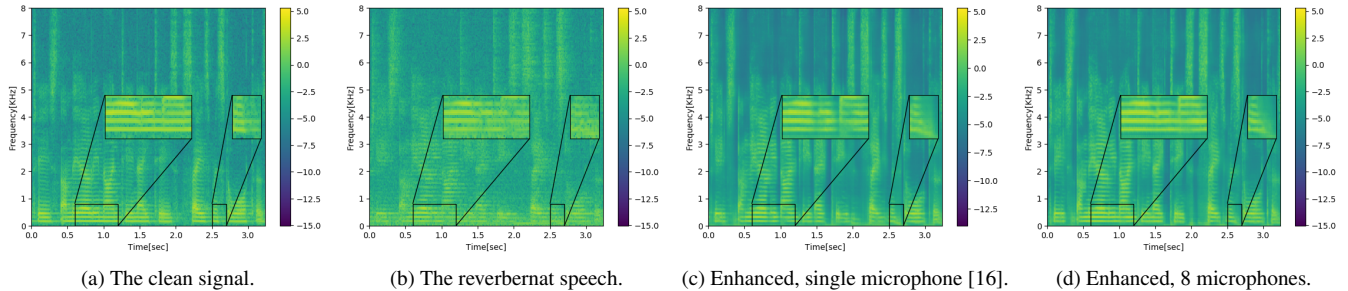
For real recordings, quantitative assessment implied that the single microphone and multi-microphone networks had comparable success, even with eight microphones. When we examined the spectrograms, we noticed that the single microphone network performed remarkably well. In order to emphasize the differences, we evaluated networks (single and multi-

Table 1: Results of simulated data for far microphones.

Room	Position-Agnostic	CD↓			PESQ↑			FWSegSNR↑		
		1	2	3	1	2	3	1	2	3
Reverberant	-	2.67	5.21	4.96	1.61	1.19	1.17	6.68	1.04	0.24
1 mic. [16]	✗	2.00	3.23	2.89	2.39	1.72	1.68	12.39	9.65	9.70
4 mics.	✗	1.70	3.11	2.70	2.51	1.80	1.72	14.45	10.32	9.58
8 mics.	✗	1.64	3.05	2.60	2.61	1.85	1.74	14.90	10.88	10.31
2 mics.	✓	1.75	3.15	2.79	2.52	1.77	1.70	14.07	10.15	9.81
4 mics.	✓	1.68	3.12	2.69	2.59	1.80	1.74	14.64	10.41	10.01
6 mics.	✓	1.65	3.01	2.61	2.59	1.87	1.77	14.79	10.72	9.96

Table 2: Results of simulated data for near microphones.

Room	Position-Agnostic	CD↓			PESQ↑			FWSegSNR↑		
		1	2	3	1	2	3	1	2	3
reverberant	-	1.99	4.63	4.38	2.14	1.4	1.37	8.12	3.35	2.27
1 mic. [16]	✗	1.64	2.48	2.41	2.97	2.40	2.20	13.76	12.33	11.64
4 mics.	✗	1.25	2.25	2.18	2.98	2.52	2.25	16.72	13.82	12.57
8 mics.	✗	1.23	2.13	2.06	3.04	2.66	2.33	17.69	14.63	13.34
2 mics.	✓	1.32	2.36	2.27	3.00	2.50	2.28	16.77	13.48	12.58
4 mics.	✓	1.28	2.24	2.17	3.07	2.59	2.31	17.29	13.97	13.10
6 mics.	✓	1.20	2.14	2.09	3.06	2.62	2.33	17.68	14.33	12.93

**Fig. 2:** Spectrograms for speech dereverberation of real recordings, far condition. The single and multi-microphone networks used 8M parameters. The eight-microphones reconstruction managed to better capture the structure of the clean log-spectrum.

microphone) that used only 8M parameters. In this case, the proposed scheme emerged advantageous, as Fig. 2 exemplifies. However, the quantitative measures still did not reflect the gap in performance. The single channel network averaged 7.71 dB and 7.04 dB of FWSegSNR for the far and near cases, respectively, while the multichannel network achieved 8.11 dB and 7.78 dB. The values for reverberant recordings were 1.20 dB and 0.43 dB, respectively. The interested reader is encouraged to listen to audio samples for both the simulated and real recordings.¹

5. CONCLUSION

We presented a neural network architecture which is oblivious to the microphone array’s position and geometry. The sug-

gested architecture builds upon the deep sets framework and DSS layers. In contrast, the common approach that concatenates the multi-microphone signals across the channel axis assumes prior knowledge on the constellation and therefore hinders its applicability to the position-agnostic setup. The new architecture was used to enhance reverberant log-spectrum from multiple noisy observations, and tested on novel train-test splits of recordings from the REVERB dataset. The objective and subjective tests showed that even though a related single-microphone technique is extremely successful, the proposed method significantly improves the performance. Moreover, our method generalises well for unseen combinations of microphones, and even improves the results with respect to setups that use the same combination during training and test stages.

¹www.eng.biu.ac.il/gannot/speech-enhancement

6. REFERENCES

- [1] A. Nábělek, T. Letowski, and F. Tucker, “Reverberant overlap - and self-masking in consonant identification,” *The Journal of the Acoustical Society of America*, vol. 86, pp. 1259–1265, Nov. 1989.
- [2] M. Kim and P. Smaragdis, “Collaborative audio enhancement using probabilistic latent component sharing,” in *IEEE International Conference on Acoustics, Speech and Signal Processing (ICASSP)*, May 2013, pp. 896–900.
- [3] P.A. Naylor and N.D. Gaubitch, *Speech Dereverberation*, Springer, 2010.
- [4] K. Kinoshita, M. Delcroix, S. Gannot, E. Habets, R. Haeb-Umbach, W. Kellermann, V. Leutnant, R. Maas, T. Nakatani, B. Raj, A. Sehr, and T. Yoshioka, “A summary of the REVERB challenge: State-of-the-art and remaining challenges in reverberant speech processing research,” *EURASIP Journal on Advances in Signal Processing*, vol. 7, pp. 1–19, 12 2016.
- [5] M. Delcroix, T. Yoshioka, A. Ogawa, Y. Kubo, M. Fujimoto, N. Ito, K. Kinoshita, M. Espi, T. Hori, T. Nakatani, and A. Nakamura, “Linear prediction-based dereverberation with advanced speech enhancement and recognition technologies for the REVERB challenge,” 2014, vol. 1, pp. 1–8.
- [6] B. Schwartz, S. Gannot, and E. A. P. Habets, “Online speech dereverberation using Kalman filter and EM algorithm,” *IEEE/ACM Transactions on Audio, Speech, and Language Processing*, vol. 23, no. 2, pp. 394–406, 2015.
- [7] B. Cauchi, I. Kodrasi, R. Rehr, S. Gerlach, A. Jukić, T. Gerkmann, S. Doclo, and S. Goetze, “Joint dereverberation and noise reduction using beamforming and a single-channel speech enhancement scheme,” May 2014.
- [8] O. Schwartz, S. Gannot, and E. A. P. Habets, “Multi-microphone speech dereverberation and noise reduction using relative early transfer functions,” *IEEE/ACM Transactions on Audio, Speech, and Language Processing*, vol. 23, no. 2, pp. 240–251, 2015.
- [9] Z. Wang and D. Wang, “Multi-microphone complex spectral mapping for speech dereverberation,” in *IEEE International Conference on Acoustics, Speech and Signal Processing (ICASSP)*, 2020, pp. 486–490.
- [10] S. Chakrabarty and E. Habets, “Multi-speaker DOA estimation using deep convolutional networks trained with noise signals,” *IEEE Journal of Selected Topics in Signal Processing*, vol. 13, pp. 8–21, Feb. 2019.
- [11] S. E. Chazan, H. Hammer, G. Hazan, J. Goldberger, and S. Gannot, “Multi-microphone speaker separation based on deep DOA estimation,” in *27th European Signal Processing Conference (EUSIPCO)*, 2019, pp. 1–5.
- [12] M. Zaheer, S. Kottur, S. Ravanbakhsh, B. Póczos, R. R. Salakhutdinov, and A. J. Smola, “Deep sets,” in *Advances in Neural Information Processing Systems 30 (NeurIPS)*, pp. 3391–3401. 2017.
- [13] Y. Luo, Z. Chen, N. Mesgarani, and T. Yoshioka, “End-to-end microphone permutation and number invariant multi-channel speech separation,” in *IEEE International Conference on Acoustics, Speech and Signal Processing (ICASSP)*, 2020, pp. 6394–6398.
- [14] Dongmei Wang, Zhuo Chen, and Takuya Yoshioka, “Neural speech separation using spatially distributed microphones,” *arXiv preprint arXiv:2004.13670*, 2020.
- [15] H. Maron, O. Litany, G. Chechik, and E. Fetaya, “On learning sets of symmetric elements,” in *International Conference on Machine Learning (ICLR)*, 2020.
- [16] O. Ernst, S. E. Chazan, S. Gannot, and J. Goldberger, “Speech dereverberation using fully convolutional networks,” in *26th European Signal Processing Conference (EUSIPCO)*, 2018, pp. 390–394.
- [17] O. Ronneberger, P. Fischer, and T. Brox, “U-net: Convolutional networks for biomedical image segmentation,” in *Medical Image Computing and Computer-Assisted Intervention (MICCAI)*. 2015, vol. 9351 of LNCS, pp. 234–241, Springer.
- [18] M. Aittala and F. Durand, “Burst image deblurring using permutation invariant convolutional neural networks,” in *The European Conference on Computer Vision (ECCV)*, Sept. 2018.
- [19] P. Isola, J. Zhu, T. Zhou, and A. A. Efros, “Image-to-image translation with conditional adversarial networks,” in *IEEE Conference on Computer Vision and Pattern Recognition (CVPR)*, 2017, pp. 5967–5976.
- [20] T. Robinson, J. Fransen, D. Pye, J. Foote, and S. Renals, “WSJCAMO: A British English speech corpus for large vocabulary continuous speech recognition,” in *International Conference on Acoustics, Speech, and Signal Processing*, 1995, vol. 1, pp. 81–84.
- [21] M. Lincoln, I. McCowan, J. Vepa, and H. K. Maganti, “The multi-channel wall street journal audio visual corpus (MC-WSJ-AV): Specification and initial experiments,” in *IEEE Workshop on Automatic Speech Recognition and Understanding.*, 2005, pp. 357–362.